8306-066

MICROALLOYING AND PRECIPITATION IN Cr-V RAIL STEELS

D. E. Parsons, T. F. Malis and J. D. Boyd
PMRL, CANMET, Energy Mines and Resources
Ottawa, Canada

A STUDY OF ALLOYING EFFECTS in Cr-V rail steels has been carried out to determine the microstructural strengthening mechanisms. The laboratory steels investigated were based on the commercial 1% Cr rail steel chemistry (0.75C - 0.8Mn - 1.25Cr - 0.30Si), and represented two levels of nitrogen (nominally 0.007 and 0.015 wt %), and two types of deoxidation practice. It is found that vanadium microalloying produces a yield stress increment of approximately 90 MPa for low nitrogen steels and 140 MPa for high nitrogen steels. This strengthening effect appears to saturate at approximately 0.15 wt % vanadium, with no further strength increase for higher vanadium concentration. The hardness and UTS exhibit the same variation with vanadium content as the yield stress. There is no consistent effect of aluminum content (deoxidation practice). Several distinct precipitate morphologies, a wide range of precipitate sizes and a non-homogeneous distribution of precipitates are observed. There is also significant partitioning of V, Cr and Mn to cementite. It is suggested that an increase in the amount of coarse, austenite-nucleated V(C,N) and possibly other coarse precipitate modes is responsible for the saturation of the vanadium strengthening effect.

INTRODUCTION

Eutectoid rail steels alloyed with chromium and vanadium have been developed which have higher hardness and better wear resistance than carbon-manganese rail, while maintaining adequate toughness, weldability and a fully pearlitic microstructure (1,2). Several metallurgical studies of the effects of composition on the microstructure and mechanical properties of Cr-V rail steels have been carried out (1-3). These investigations confirm the positive strengthening effect of microalloying with vanadium, but they give conflicting results for the relationship between yield stress and vanadium content. Evidence for vanadium carbide precipitates in such steels has been produced by transmission electron microscopy (2,4), but the details of the precipitation process are not known. In particular, it would be advantageous to understand the relationships between composition, processing variables and V(C,N) precipitation to optimize the properties of Cr-V rail steels. For instance, studies of the effects of cooling rate following rolling in C-Mn-V eutectoid steels indicate that maximum precipitation strengthening occurs at rates of $5°C.s^{-1}$ (5), i.e., approximately 10 times faster than normal rail-head cooling rates.

In the present study, the effects of vanadium, nitrogen and aluminum contents were investigated for a series of C-Mn-Cr-based rail steels, produced by a processing route designed to simulate standard rail production. The objectives were to determine the compositional dependence of the mechanical properties, to characterize the microstructures in detail, and to identify the microstructural strengthening mechanisms.

EXPERIMENTAL

A series of experimental steels, based on commercial 1% Cr rail-steel chemistry (0.75C - 0.8Mn - 1.25Cr - 0.30Si), was prepared as 225 kg heats by air-induction melting with argon cover. Each heat was tapped into a ladle, and cast as four 125 mm x 125 mm x 380 mm rectangular blocks. After the first two blocks of each heat were poured, aluminum was plunged into the ladle, and the remaining two blocks were poured. The compositions of the experimental steels given in Table 1 are the average values for the two blocks of each steel. With the exception of nitrogen, all of the analyses were carried out by direct-reading spectrometer. Total nitrogen contents were determined by a modified Kjeldahl distillation method, and the results were confirmed by analysing selected specimens using a LECO nitrogen analyser. The experimental steels represented (i) two levels of nitrogen by wt %; (low) L - 0.004/0.010 and (high) H - 0.011/0.022; (ii) a range of vanadium contents from 0-0.33;

Table 1: Compositions of experimental steels (wt %)

Steel	C	Mn	Si	S	P	Cr	V	Al	N
L1	0.74	0.92	0.28	0.031	0.011	1.24	-	0.006	0.008
L2	0.74	0.90	0.27	0.029	0.011	1.21	-	0.078	0.004
L3	0.78	0.87	0.27	0.030	0.013	1.20	0.14	0.008	0.007
L4	0.79	0.87	0.27	0.032	0.014	1.20	0.14	0.058	0.007
L5	0.73	0.81	0.30	0.008	0.015	1.28	0.23	0.005	0.005
L6	0.74	0.80	0.30	0.009	0.014	1.29	0.23	0.080	0.008
L7	0.69	0.87	0.28	0.025	0.012	1.21	0.30	0.011	0.010
L8	0.69	0.85	0.28	0.024	0.013	1.21	0.30	0.062	0.010
H1	0.74	0.85	0.30	0.038	0.011	1.23	-	0.008	0.022
H2	0.77	0.84	0.31	0.030	0.015	1.25	-	0.070	0.021
H3	0.80	0.89	0.32	0.013	0.014	1.15	0.16	0.013	0.011
H4	0.74	0.83	0.30	0.030	0.017	1.23	0.16	0.040	0.015
H5	0.80	0.86	0.33	0.015	0.014	1.23	0.33	0.008	0.020
H6	0.81	0.86	0.32	0.015	0.014	1.23	0.33	0.088	0.020

and (iii) silicon deoxidation practice and deoxidation with silicon and aluminum.

One hundred and twenty five millimetre thick slabs of each steel were soaked at 1260°C for 2 h and rolled to 25 mm thick plate, finishing at 1060°C. The temperature of the work piece was monitored during rolling and cooling by two thermocouples imbedded 76 mm from each end of the slab. After rolling, the plates were controlled cooled such that one end cooled at $0.55°C.s^{-1}$ to simulate the normal rail-head hot-bed cooling rate, and the other end cooled in air at $0.77°C.s^{-1}$. Specimens for metallographic examination, hardness and tensile tests were taken from the regions adjacent to the thermocouples, for which the cooling rates were accurately known.

Longitudinal tensile specimens were tested for each plate. Hardness tests and microstructural studies were made on longitudinal sections. The microstructure was characterized by optical and scanning electron microscopy (SEM). Specimens for transmission electron microscopy were prepared from steels H4 (0.16V, 0.015N) and H6 (0.33V, 0.020N) in the form of 3 mm self-supporting discs, spark-machined from 60 μm sheet, and electropolished in 5% $HClO_4$, 15% 2-butoxyethanol, 80% methanol @ -40°C. They were examined in a fully analytical Philips EM400T scanning transmission electron microscope (TEM/STEM), with an EDAX 9100/60 EDS microanalysis system.

RESULTS

Unless stated otherwise, all of the results pertain to the plates cooled at $0.55°C.s^{-1}$. The tensile properties and hardnesses for all the steels are given in Table 2. The data reported are the average values of tests on the duplicate blocks of each steel. The variation in the 0.2% yield stress and hardness with vanadium content is shown in Fig. 1.

It is evident that the vanadium microalloy additions produce yield stress increments of approximately 90 MPa for the low-nitrogen steel (L) and approximately 140 MPa for the high-nitrogen steels (H). This strengthening effect appears to saturate at approximately 0.15 wt % vanadium, with no further increase in yield stress at higher vanadium concentrations. There is no consistent effect of aluminum content (deoxidation practice). The hardness and UTS exhibit the same variation with vanadium as the yield stress.

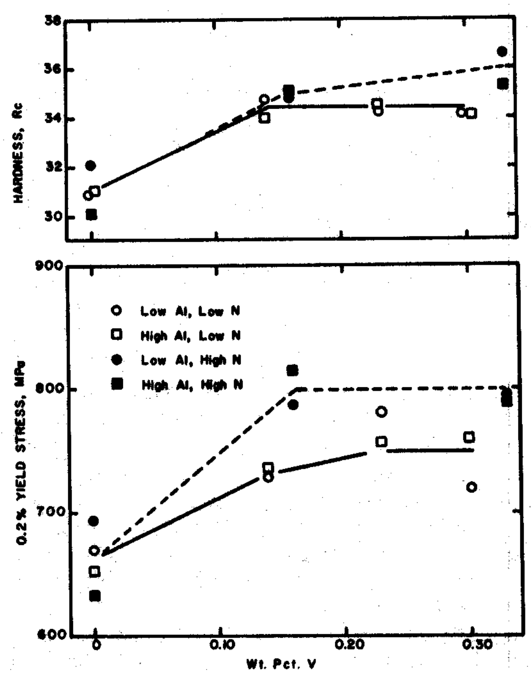

Fig. 1. Variation in yield stress and hardness with vanadium content.

Table 2: Tensile properties and hardness of rolled plates

Steel	0.2% Yield stress, MPa	UTS, MPa	% Elong (in 50 mm)	% Red. in area	Hardness, Rc ($0.55°C.s^{-1}$)	Hardness, Rc ($0.77°C.s^{-1}$)
L1	670	1132	8	16	30.9	33.0
L2	652	1111	8	16	31.0	32.5
L3	728	1208	7	14	34.8	36.3
L4	735	1214	7	15	34.0	35.7
L5	780	1221	7	19	34.3	36.1
L6	756	1197	9	21	34.5	36.3
L7	718	1173	10	24	34.1	35.9
L8	759	1194	11	27	34.1	35.5
H1	694	1149	8	20	32.1	32.4
H2	632	1104	9	23	30.2	30.8
H3	787	1249	7	15	34.8	36.3
H4	814	1221	9	20	34.9	35.7
H5	797	1263	7	15	36.6	37.5
H6	791	1273	8	15	35.3	36.7

The microstructure of the steel is fully pearlitic (Fig. 2 and 3). The pearlite is predominantly lamellar, although there are areas of degenerate pearlite. The prior austenite grain size appears to be larger for the base composition (L1) compared with the other compositions. Apart from that, there is no significant difference in prior austenite grain size, pearlite colony size or pearlite interlamellar spacing for all of the steels investigated.

There is a wide range of pearlite interlamellar spacings within each steel. From measurements made on SEM photographs of 10 fields of steel H4, selecting areas where the lamellae were nearly perpendicular to the plane of observation (e.g., Fig. 3a), the mean minimum pearlite spacing was determined to be 170 ± 20 nm.

The vanadium-bearing steels contain fine precipitates predominantly in the pearlitic ferrite (Fig. 4-6). Dark-field imaging of these small particles was aided immensely by use of a conical dark field mode in the Philips Hybrid Diffraction Module. Briefly, this allows scanning of every diffraction pattern reflection in a matter of minutes and waiting for the precipitates to "light up".

Several distinct precipitate morphologies, a wide range of precipitate sizes, and a non-homogeneous distribution of precipitates is observed. Figure 4 illustrates the three most common precipitate morphologies: (i) small (~5 nm), discrete particles, relatively uniformly distributed in the ferrite, often with a precipitate-free zone adjacent to cementite lamellae (Fig. 4a); (ii) larger (30-50 nm), discrete particles, having a much lower volume fraction than the small precipitates (Fig. 4b); (iii) short rows of precipitates which appear to be heterogeneously nucleated on dislocations (Fig. 4c). Figure 5 shows two types of precipitate morphologies in the same area, as revealed by different precipitate reflections. The dislocation-nucleated particles can join to form continuous rods of particles, that can extend into the cementite (Fig. 6a), and there is evidence of preferential nucleation at the ferrite-cementite interface (Fig. 6b). The density of precipitation is quite variable, even within one pearlite colony. There are many areas devoid of precipitates, in addition to those with the precipitate distributions shown in Fig. 4-6. In some areas, the distribution of a single variant of precipitates shows no relationship to the pearlite structure, indicating nucleation in the austenite.

X-ray microanalysis was conducted under as nearly-identical conditions as possible (operating voltage, tilt angle, proportionality factors for quantitative analysis, and spectrum acquisition and processing parameters). Thin foil thicknesses were estimated from contamination spots, then absorption and flourescence corrections were made. Thus, comparative quantification between either thin foil or bulk analyses performed under the same operating conditions should be accurate to within ±5% or less. Three points emerged from the microanalysis data:

(a) the bulk analysis of several areas a few microns square within large regions (30 x 40 µm) covering several different pearlite colonies, showed no substantial composition differences within or between colonies in either low- or high-V steels. There was some suggestion of slight differences across prior austenite boundaries;

(a)

40 μm

(b)

(c)

(d)

Fig. 2. Representative optical micrographs (2% nital etch). (a) L1, (b) L6, (c) H2, (d) H6.

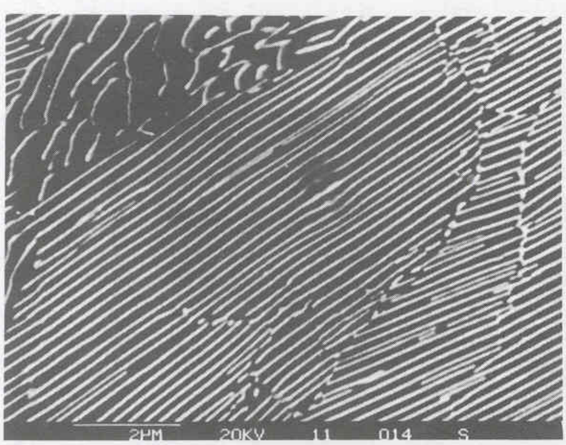

(a)

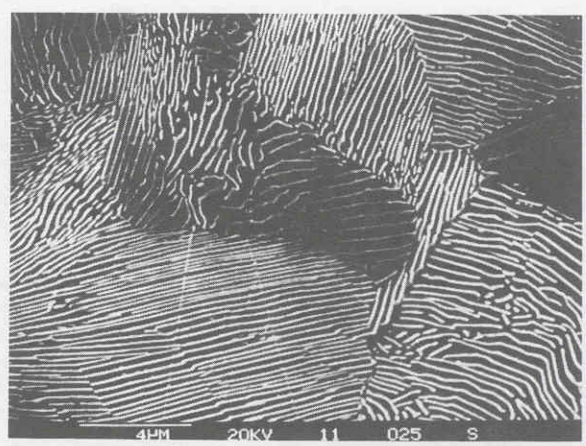

(b)

Fig. 3. Scanning electron micrographs of etched specimens (2% nital). (a) H4, (b) H6.

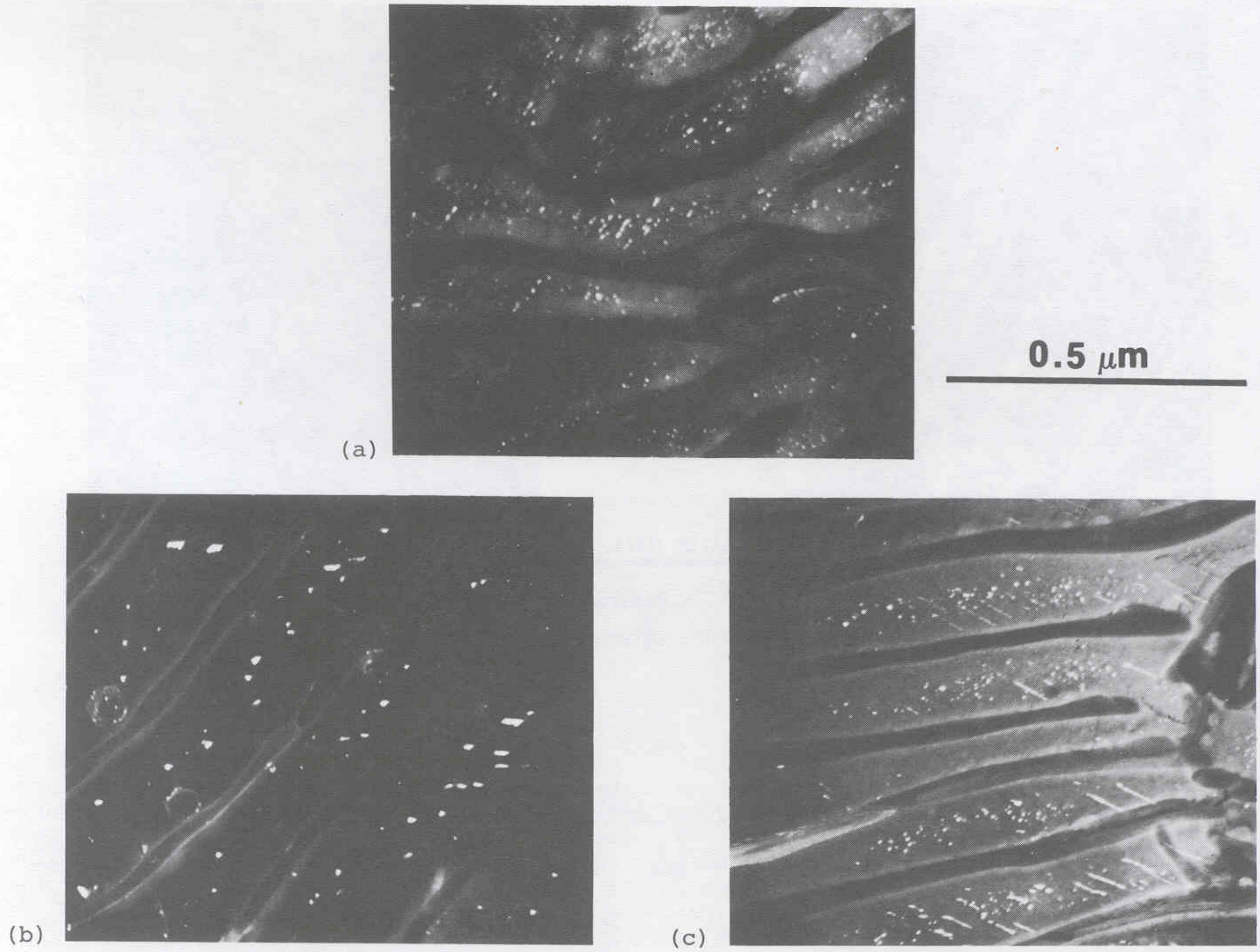

Fig. 4. H4, dark-field transmission electron micrographs, illustrating different precipitate morphologies.

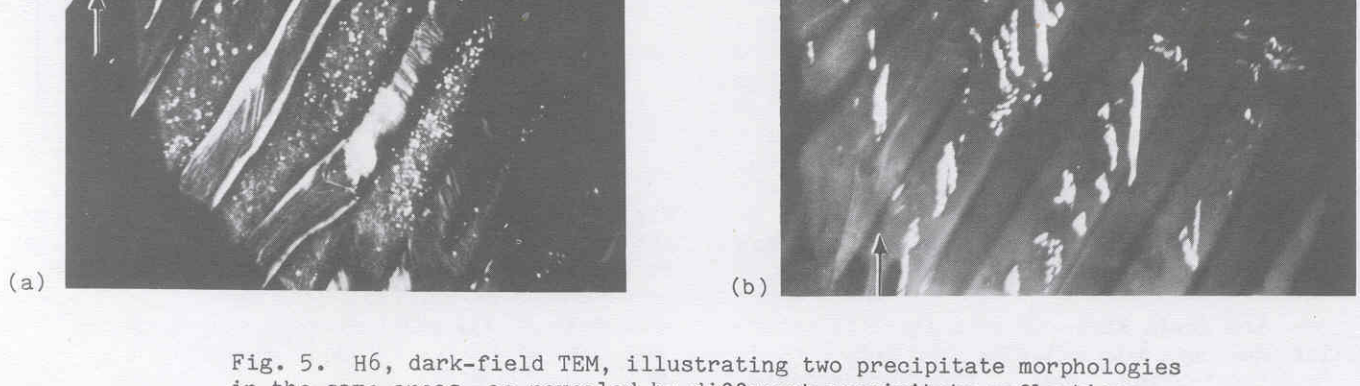

Fig. 5. H6, dark-field TEM, illustrating two precipitate morphologies in the same areas as revealed by different precipitate reflections.

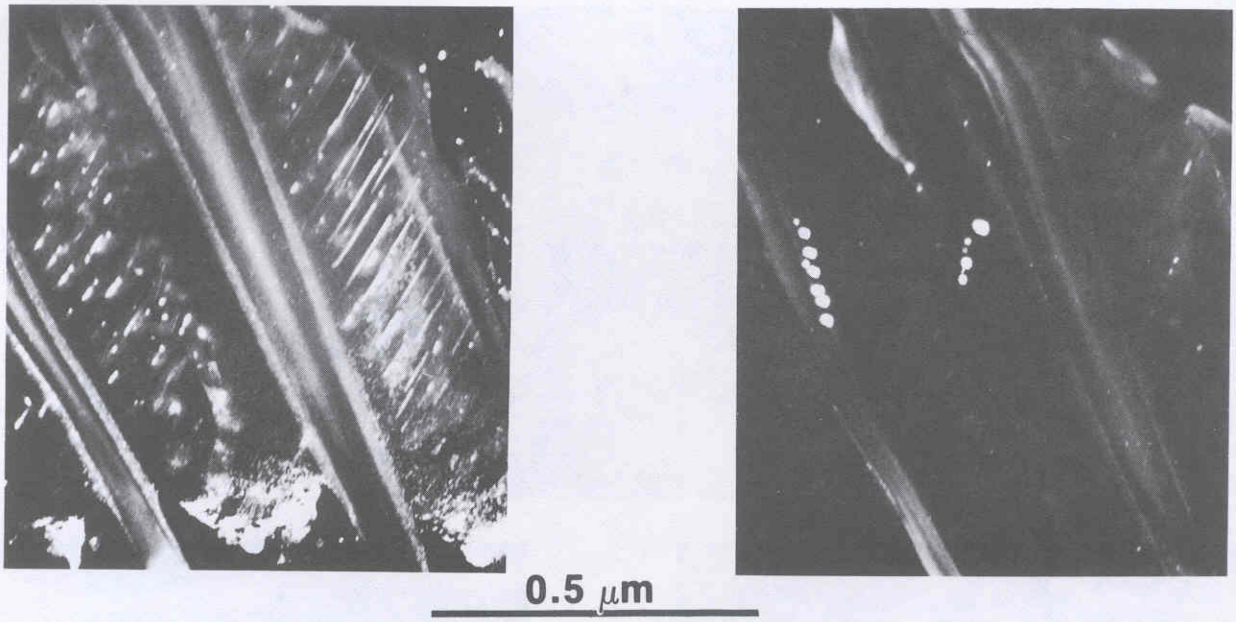

Fig. 6. H6, dark-field TEM, illustrating different morphologies of heterogeneously nucleated precipitates.

(b) there was a marked partitioning of V, Cr and Mn from the ferrite to the cementite in both low- and high-V steels. Fine probe analysis of cementite lamellae sticking out from the edges of the electron transparent region made the analyses quite accurate. They showed a tenfold enhancement of V and Cr and a fivefold enhancement of Mn. This partitioning occurred for all lamellae examined, irrespective of whether or not ferrite precipitation was present nearby.

(c) all the precipitate morphologies described were seen to be V rich under very fine beam (10 nm) microanalysis conditions, indicating they were V(C,N). The exact composition of the precipitates was not determined.

DISCUSSION

The yield stress increments resulting from vanadium microalloy additions found in the present work are comparable to the values reported elsewhere (1-5). Some published values of yield stress as a function of vanadium content are compared with the present results in Fig. 7. The agreement is reasonable considering the variations in composition and processing schedules for the different steels. The general result is that vanadium microalloying produces a maximum yield stress increment of 100-150 MPa, which occurs at approximately 0.15V, with no further increase for higher vanadium contents.

Since the grain size and mean pearlite interlamellar spacing is essentially the same for all the vanadium-bearing steels, the strengthening mechanism must be the precipitation of V(C,N) in the pearlitic ferrite. Calculations of the precipitation strengthening component from measurements of precipitate sizes and volume fractions in a similar steel cooled at the same rate give a value of 70 MPa (6). However, not all of the

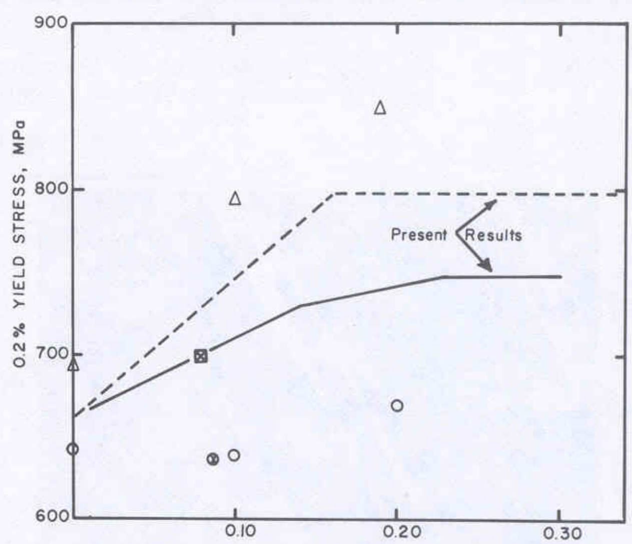

Fig. 7. Comparison of published data with present measurements of yield stress as a function of vanadium content.

△ - Parsons et al. (3),
○ - Sage et al. (2) (laboratory steels)
⊗ - Sage et al (2) (production heat)
⊠ - Schmedders (1)

vanadium precipitates as a fine dispersion of V(C,N) particles. The present results show clearly that there are coarse V(C,N) precipitates, decorated dislocations, interphase precipitates and vanadium solute partitioning to cementite. Vanadium partitioning to cementite has been reported elsewhere (7,8), but this is the first observation of the heterogeneously nucleated V(C,N) precipitates. No consistent effect of total vanadium content on any of these vanadium sites has been established. The specimens examined appear to show more austenite-nucleated precipitates with increasing vanadium content. It is suggested that the increase in the amount of coarse, austenite nucleated V(C,N) and possibly other coarse precipitate modes is responsible for the saturation of the vanadium strengthing effect around 0.15V.

Other work has shown that a finer distribution of precipitates and a larger precipitation strengthening component occur at higher cooling rates (5,7). The increased cooling rate would lower the transformation temperature (from ~700°C for the present steels), suppress V(C,N) nucleation in the austenite and V partitioning to cementite, and produce a higher volume fraction of fine precipitate in the ferrite. The lack of influence of Al content is consistent with data for low C steels (9). In the TEM specimens of H4 and H6, very few AlN cuboids were seen. Those that were observed were of the order of a micron in size, which is too large for any strengthening effect.

As seen in Fig. 1, there is a yield stress increment of approximately 50 MPa at the high N level. This may be a function of more V being involved in precipitation than in partitioning to cementite, and is being investigated currently.

CONCLUSIONS

Vanadium microalloying produces a yield stress increment of 100-150 MPa, which saturates at approximately 0.15 wt % vanadium. There is a similar variation in UTS and hardness with vanadium content.

There is no consistent effect of aluminum content (deoxidation practice) on the microstructure or tensile properties.

The strengthening effect is due to fine (30-50 nm) V(C,N) precipitates. However, there are also coarse V(C,N) precipitates resulting from precipitation in austenite, interphase precipitation and nucleation of precipitates on dislocations.

There is significant partitioning of vanadium, chromium and manganese to cementite.

It is suggested that modifications to the processing schedule (e.g. accelerated cooling) would achieve a more effective utilization of vanadium by producing a higher volume fraction of fine precipitates in the ferrite.

ACKNOWLEDGEMENTS

The authors would like to thank L. Seto and A. Euser for their technical assistance.

REFERENCES

1. Schmedders, H., Vanadium in Rail Steels, p. 3, VANITEC, London (1979)

2. Sage, A.M., W. Hodgson and D.H. Stone, ibid, p. 12.

3. Parsons, D.E., D.A. Munro and J. Ng-Yelim, "Vanadium-Modification of Two Premium Rail-Steel Compositions", Can. Met. Quart. (in press)

4. Heller, W., R. Schweitzer and L. Weber, Can. Met. Quart. 21, 3-15 (1982)

5. Ridley, N., M.T. Lewis and W.B. Morrison, "The Effect of Small Additions of Vanadium on the Strength of Pearlitic Steels", Advances in the Physical Metallurgy and Applications of Steels, Metals Society, London, Book No. 284 (1982)

6. Laufer, E.E. and D.M. Fegredo, "A Quantitative Electron Microscopic Examination of Nb- and V(C,N) Precipitates in Eutectiod Premium Rail Steels Transformed Under Various Conditions", Can. Met. Quart 22 (1983) (in press)

7. Dunlop, G.L., C.-J. Carlsson and G. Frimodig, Met. Trans. 9A, 261-266 (1978)

8. Mottishaw, T.D. and G.D.W. Smith, "Microalloyed Pearlitic Steels for the Wire Industry: Mechanisms of Alloy Element Redistribution and Strengthening Processes in Cr-V Eutectoid Steels", this conference.

9. Heikkinen, V.K. and J.D. Boyd, Can. Met. Quart. 15, 219-226 (1976)